Journal Pre-proofs

Differential regional pectoralis major activation indicates functional diversity in healthy females

Tea Lulic-Kuryllo, Francesco Negro, Ning Jiang, Clark R. Dickerson

PII: S0021-9290(22)00024-0
DOI: https://doi.org/10.1016/j.jbiomech.2022.110966
Reference: BM 110966

To appear in: *Journal of Biomechanics*

Received Date: 15 March 2021
Revised Date: 13 January 2022
Accepted Date: 17 January 2022

Please cite this article as: T. Lulic-Kuryllo, F. Negro, N. Jiang, C.R. Dickerson, Differential regional pectoralis major activation indicates functional diversity in healthy females, *Journal of Biomechanics* (2022), doi: https://doi.org/10.1016/j.jbiomech.2022.110966

This is a PDF file of an article that has undergone enhancements after acceptance, such as the addition of a cover page and metadata, and formatting for readability, but it is not yet the definitive version of record. This version will undergo additional copyediting, typesetting and review before it is published in its final form, but we are providing this version to give early visibility of the article. Please note that, during the production process, errors may be discovered which could affect the content, and all legal disclaimers that apply to the journal pertain.

© 2022 Published by Elsevier Ltd.

The final publication is available at Elsevier via http://dx.doi.org/10.1016/j.jbiomech.2022.110966. © 2022. This manuscript version is made available under the CC–BY–NC–ND 4.0 license http://creativecommons.org/licenses/by–nc–nd/4.0/

Differential regional pectoralis major activation indicates functional diversity in healthy females

Original Article: *Journal of Biomechanics*

Tea Lulic-Kuryllo[1], Francesco Negro[2], Ning Jiang[3], Clark R. Dickerson[1*]

[1]Department of Kinesiology, University of Waterloo, Waterloo, Canada

[2]Department of Clinical and Experimental Sciences, Universita degli Studi di Brescia, Brescia, Italy

[3]Department of Systems Design Engineering, University of Waterloo, Waterloo, Canada

*Corresponding author:
Clark R. Dickerson
Department of Kinesiology
Faculty of Applied Health Sciences
University of Waterloo
200 University Avenue West
Waterloo, ON N2L 3G1, Canada
E-mail: cdickers@uwaterloo.ca
Phone: +1 519-888-4567 x37844
Fax: +1 519-746-6776

Abstract Word Count: 248

Main Text Word Count: 3989

Number of Figures: 6

Keywords: *high-density electromyography, shoulder, muscle activation, female health*

Journal Pre-proofs

ABSTRACT

Pectoralis major activation enables the performance of several upper extremity movements. Its regional activation, however, is not documented in healthy females. This work used high-density surface electromyography to investigate regional pectoralis major activation in twenty-nine healthy young females across two independent experiments in several ramp and hold isometric tasks and force levels. Regional mean root mean square amplitudes (normalized to the task-specific maxima) were quantified for the clavicular, superior, and middle sternocostal regions. Two-way ANOVAs were used to determine if differences in normalized regional activation exist within each task and force level. The middle sternocostal region activated 12-108% more than the clavicular and the superior sternocostal region in extension, adduction with external rotation, and high elevation internal rotation. In high elevation adduction, the middle sternocostal region activated more (7-22%) than the superior sternocostal region. In low elevation, internal rotation (60°), the clavicular and middle sternocostal regions activated more (9-13%) than the superior sternocostal region, while in adduction 60°, the clavicular region activated 9-19% more than the superior sternocostal region. Lastly, in forward and horizontal flexion, all three regions activated similarly irrespective of the force level, except at 25% MVF in forward flexion, where the clavicular region activated 21% more than the superior sternocostal region. This work provides a first comprehensive evaluation of the normalized regional pectoralis major activation in healthy females. The present findings indicate that the performance of isometric tasks in different directions activates different pectoralis major regions in healthy females, suggesting regional specificity to functional actions.

Journal Pre-proofs

INTRODUCTION

Several shoulder muscles, including the morphologically complex pectoralis major, coordinate to enable arm function. Comprised of two anatomically distinct regions (Ashley, 1952; Fung et al. 2009; Lewis 1901; Wolfe et al. 1992), pectoralis major activation enables upper extremity movement in several directions (Ackland et al. 2008; Ackland and Pandy, 2011). Specifically, the clavicular region assists in humeral flexion and internal rotation, while the sternocostal region contributes to humeral adduction, internal rotation, and extension against resistance (Ackland et al. 2008; Ackland and Pandy, 2011; Wolfe et al. 1992).

Current knowledge on regional pectoralis major activation only exists for healthy males (Brown et al. 2007; Paton and Brown, 1994; Wickham et al. 2004), although clinical and training contexts may necessitate sex-specific recommendations. For example, greater age-related changes in the role and utilization of pectoralis major regions occurred in females (Setlock et al. 2021). Secondly, some breast reconstruction procedures, such as the subpectoral flap, disinsert the pectoralis major from the ribs to accommodate an implant, thereby altering regional pectoralis major mechanical properties (Leonardis et al. 2019). Third, the pectoralis major is targeted in several athletic and strength training activities, such as the bench press (Cabral et al. 2021). Current recommendations for these exercises rely on male-specific activation patterns, as regional female patterns lack documentation. Thus, uneven training adaptations may occur for females.

Pectoralis major activation is typically evaluated using surface electromyography (sEMG), often classic, low-spatial resolution bipolar sEMG, which is limited. Classic bipolar sEMG samples from a spatially small area of the muscle, failing to capture whole muscle activation, especially in large muscles such as the pectoralis major (Lulic-Kuryllo et al. 2021). In contrast, novel high-density sEMG (HD-sEMG) overcomes this limitation by sampling from an array of

electrodes spanning the muscle. This is critical in female data due to breast tissue overlying the middle-to-lower sternocostal regions.

Therefore, the present work purposed to evaluate regional pectoralis major activation in healthy females using HD-sEMG in several functionally relevant tasks across varying force levels. Based on prior isometric task evaluations in healthy males (Brown et al. 2008; Paton and Brown, 1994; Wickham et al. 2004), several hypotheses emerged: 1) the middle sternocostal region would be more activated than the other regions in extension and adduction tasks across all force levels, 2) the clavicular region would be more activated in forward flexion, and 3) the clavicular and superior sternocostal regions would be more activated in horizontal flexion. Despite a lack of prior study of internal rotation data, based on anatomical moment arm data (Ackland and Pandy, 2011), the middle sternocostal region would hypothetically activate more than the other regions.

METHODS

Participants

This work consisted of two independent experiments. Twenty (22.4 ± 2.2 years) and nine (24.5 ± 3.1 years) healthy, right-hand dominant, recreationally active young females participated. All participants were free from low back pain in the past six months, musculoskeletal injuries, or neurological disease. None had previous breast reconstruction or augmentation surgery or tested positive for impingement signs, as determined by Hawkin's impingement and Apley's Scratch test. All participants wore a regular bra (i.e., no sports bra) to allow for array placement over the muscle without compressing the HD-sEMG arrays and were instructed to refrain from engaging in strenuous physical activity at least 24 hours before the session to mitigate potential subsequent day muscle fatigue. Both studies received ethics clearance by the institutional office of research ethics,

and all participants provided informed consent. Clavicle length was measured from the acromion to the sternal notch, while the sternal length was measured from the sternal notch to the palpated xiphoid process, both with a measuring tape.

High-density surface electromyography

A single high-density surface electromyography (HD-sEMG) array consisting of 64 electrodes in an 8 by 8 matrix with a 10 mm inter-electrode distance was used to acquire EMG from the right pectoralis major in monopolar mode (ELSCH064NM3, SpesMedica, Italy; **Figure 1A**). The HD-sEMG array was placed ~2 cm inferior to the clavicle, with the middle of an array positioned between the sternum and the axilla and parallel to the muscle fibers. The array was fixed with adhesive tape and connected to a 64 channel EMG amplifier (EMGUSB2+, OTBioelecttronica, Torino, Italy). Before applying the array, the skin was cleaned with abrasive paste and water. The HD-sEMG array holes were filled with electroconductive gel, and the array was applied on the skin using a 1 mm thick two-sided adhesive foam. All EMG signals were bandpass filtered with a cut-off frequency between 10 – 500 Hz and sampled at 2048 Hz with a 12-bit A/D converter (5V dynamic range). HD-sEMG signals were amplified by a factor between 100-5000 V/V, which was accounted for in the post-processing steps. One wet patient reference electrode was wrapped around the participant's right wrist, while another monopolar reference electrode was placed on the right clavicle as per device requirements to reduce power line interference.

Electrocardiography measurement (ECG)

Electrocardiography (ECG) was acquired concurrently with HD-sEMG using Ag\AgCl disposable electrodes in a monopolar configuration. The purpose of ECG collection was to remove the heart rate from HD-sEMG signals in post-processing steps. Three electrodes were placed over

the left chest at the 6th costal level, approximately along the anterior axillary line, and medially at the sternocostalis junction (Drake and Callaghan, 2006). Before the placement of the electrodes, the area was cleaned with abrasive gel and water. ECG was collected using a wireless telemetered system (Noraxon Telemyo 2400 T G2 Noraxon, Arizona, USA). Raw signals were band-pass filtered from 10-1000 Hz and differentially amplified with a common-mode rejection ratio of more than 100dB and an input impedance of 100 MΩ. Analog signals were converted to digital using a 16-bit A/D card with a ±10 V range. The sampling frequency was 1500 Hz.

Force

Raw voltages in X, Y, and Z directions were acquired concurrently with HD-sEMG and ECG. Participants exerted force against a custom-built arm-cuff (shown in **Figure 2**) attached to a six-degree-of-freedom force transducer (MC3A, AMTI MA, USA) mounted on a robotic arm (**Figure 2**; Motoman Robotics Division, Yaskawa America, USA). The transducer's sampling rate was set to 1500 Hz and amplified (1000x) using VICON Nexus 1.7.1 software.

Experimental protocols

The protocols involved task-specific maximal voluntary (MVF) and submaximal ramp-and-hold isometric tasks at specified force levels. All participants underwent a brief warm-up and training, which involved performing ramp-and-hold submaximal tasks with visual feedback of the exerted force. The training familiarized the participant with each task, the setup, and preconditioned the muscle-tendon unit (Maganaris et al., 2002). The participant sat on a chair with an upright torso secured using a padded strap to mitigate trunk movement. All tasks were performed against an arm-cuff with visual feedback of the participant's exerted force provided on

a monitor. Following practice, participants performed two trials of task-specific 5-second MVFs. These tasks were examined in Experiment 1 (**Figure 2A**): a) adduction and b) internal rotation at 60° of arm abduction; c) adduction at 90º of arm abduction; and d) adduction at 90º of arm abduction and 90º of arm external rotation (adduction external 90); and Experiment 2 (**Figure 2B**): a) extension at 20° of abduction; b) forward flexion at 20° of abduction; c) horizontal flexion at 90° of abduction and 50° of flexion in the transverse plane, and d) internal rotation at 90° of abduction and 20° of internal rotation. The chosen tasks typically require pectoralis major to act as a prime mover, synergist, or antagonist (Wickham et al. 2012). During MVF performance, the investigators verbally encouraged participants. Each MVF was separated by 2 minutes of rest. MVF values were quantified using a custom-made LabVIEW program (National Instruments). The mean of the two task-specific MVF trials was used to scale all submaximal trials within that task.

Participants performed several submaximal ramped and hold isometric tasks (**Figure 1B**) scaled to 15%, 25%, 50%, or 75% MVF. The range of force levels reflects a range of muscular responses observed in typical daily, occupational, and exercise tasks. Tasks and force levels were block randomized between and within participants. Each trial within a force level was performed twice consecutively. Trials lasted 60 seconds for 15% and 25% MVF, 30 seconds for 50% MVF, and 10 seconds for 75% MVF. Minimum three to five-minute rest breaks interposed trials. During MVF and submaximal trial performance, participants were required to exert force in the primary axis direction for that task. If large off-axis forces were detected, the trial was stopped, the task verbally described to the participant, and the trial repeated. These occurrences were minimal due to the precedent training.

Journal Pre-proofs

Data Analysis

HD-sEMG signal processing

Before analyses, HD-sEMG signals for each channel were inspected for artifacts using a custom-made Matlab program (Matlab 2019b; Mathworks, Inc.). A channel was removed if it contained movement artifacts, saturated, or had insufficient skin contact (i.e., no signal detected). These channels were subsequently interpolated in data analyses. Further, the differential amplitude of the HD-sEMG signals across channels was comparable to baseline EMG levels in extension and internal rotation 90° at 15% MVF across all participants, prompting the removal of this force level from further analyses for these tasks. Lastly, any trials with substantial saturation, artifacts, or low electrode-skin contact were removed from subsequent analyses (~1.2% of the trials). An external trigger that depolarized to 5 Hz at the beginning of the trial was used to sync the HD-sEMG signals, ECG, and force.

Before signal processing, ECG was used to eliminate heart rate contamination from monopolar HD-sEMG signals. Specifically, the ECG was interpolated to 2048 Hz, and the HD-sEMG signals were cross-correlated with the heart rate to match the timing of each heartbeat's peak amplitude. Each trial was visually inspected to make sure the algorithm correctly recognized the ECG peaks. The precise timing of each ECG peak was determined, and only the frames corresponding to the ECG peaks were removed from the quantification of the root mean square (RMS) amplitude.

Raw HD-sEMG data were band-pass filtered with a 3rd order Butterworth filter (20-500 Hz). The differential derivation was quantified from left to right (i.e., from axilla towards sternum), resulting in 56 channels after differentiation. The root mean square (RMS) values were computed from each of the 56 channels with a 0.25 second nonoverlapping RMS window. The resultant force

was used as a reference to analyze only the first half of the hold. The most stable part of the resultant force was selected by dividing the force signal into 5-second segments and performing the analyses on the segment with the lowest coefficient of variation. All submaximal data were normalized to maximal trials. For each HD-sEMG channel within an MVF, a mean of a 3-second window surrounding the maximal force was extracted. Following this, each channel within a submaximal trial was normalized to the channel and task-specific maximal value. Since the pectoral area differs in size across participants, a scaling factor was applied separately for each participant to allow for HD-sEMG data to be combined from all participants and ensure the same regions are included in the analyses. As such, normalized EMG amplitude data were defined in an individual pectoral system by scaling each participant's spatial map to the participant whose clavicle and sternal length were the longest. Following scaling, the superior HD-sEMG array was divided into clavicular (rows 1-2), superior (rows 3-5), and middle sternocostal (rows 6-8) regions, and the mean for each region was quantified (**Figure 1A**). This division was based on the regional anatomical descriptions defined by (Fung et al., 2009). Subsequently, the regional mean of the two trials within each task and force level was quantified.

Force processing

Raw voltage collected in submaximal and maximal trials was low pass filtered using a 3rd order Butterworth filter with a cut-off frequency of 15 Hz and converted to Newtons using a custom-made Matlab program. The mean force that matched the most stable part of the resultant force (i.e., same as for the HD-sEMG analyses) was quantified for all submaximal trials and normalized to the task-specific MVF. Normalized force data was used to confirm correct force levels for all submaximal task trials.

Statistical Analyses

All statistical analyses were performed in SPSS (IBM, version 21). Initially, the data were checked for normality and sphericity using the Shapiro-Wilk test and Mauchly's test of sphericity, respectively. Data across all tasks were not normally distributed and were *log*-transformed. Two-way repeated-measures analysis of variance (ANOVA) was performed on normalized EMG amplitude for each task with within-subject factors *Region* (clavicular, superior, and middle sternocostal) and *Force Level* (15%, 25%, 50%, or 75% MVF). Significance level for all tests was $p < 0.05$. If significant interactions between *Region* and *Force Level* existed, planned comparisons with a Bonferonni correction determined significant differences between regions within a force level ($p < 0.016$).

RESULTS

All participants maintained exerted forces within 4% of the target. Spatial activation maps in **Figures 3** and **4** show high normalized activation of the middle sternocostal region in internal rotation 90, adduction 90, adduction with external rotation, and extension. Specifically, in internal rotation 90, a main effect of *Region* occurred ($F_{2,16} = 24.6$, $p < 0.0001$, $\eta^2p = 0.75$). The middle sternocostal region had 14% higher normalized EMG amplitudes than the clavicular ($p = 0.002$) and 24% higher normalized EMG amplitudes than the superior sternocostal region ($p < 0.001$; **Figure 3A**). No differences existed between clavicular and superior sternocostal regions ($p = 0.04$). In adduction 90, an interaction between the *Region* and *Force Level* existed ($F_{2.4, 43.9} = 3.6$, $p = 0.027$, $\eta^2p = 0.16$). The middle sternocostal consistently activated more than the superior sternocostal region (15% MVF: $p < 0.001$; 25% MVF: $p = 0.001$; 50% MVF: $p = 0.012$), but not the clavicular region (all $p > 0.016$; **Figure 3B**). No differences in normalized EMG amplitudes

existed between the clavicular and superior sternocostal regions (all $p > 0.016$). Similarly, an interaction between the *Region* and *Force Level* existed in adduction 90 external 90 ($F_{1.8, 32.7} = 4.1$, $p = 0.028$, $\eta^2p = 0.18$). The middle sternocostal region activated between 12% and 42% more than the clavicular (15% MVF: $p < 0.001$; 25% MVF: $p = 0.001$; 50% MVF: $p = 0.007$) and 19% to 44% more than the superior sternocostal region (all $p < 0.001$; **Figure 4A**). No differences in existed between the clavicular and superior sternocostal region (all $p > 0.016$). Finally, in extension, the middle sternocostal region normalized EMG amplitude was ~2 times greater than the clavicular and superior sternocostal region for all force levels (*Region* by *Force Level*: $F_{1.77,14.1} = 12.6$, $p = 0.001$, $\eta^2p = 0.61$; all $p < 0.016$; **Figure 4B**). The clavicular and the superior sternocostal regions activated to the same degree across all force level (all $p > 0.016$).

In contrast, the clavicular and the middle sternocostal regions activated highly in internal rotation 60 and adduction 60 (**Figure 5)**. In internal rotation, a *Region* by *Force Level* interaction existed ($F_{2.5, 43.1} = 4.77$, $p = 0.008$, $\eta^2p= 0.21$). The clavicular and middle sternocostal regions activated more than the superior sternocostal region at 25% and 50% MVF (all $p < 0.016$; **Figure 5A**). At 15% MVF, clavicular region activated more than the superior sternocostal ($p < 0.0001$), but not the middle sternocostal region ($p = 0.02$). No differences existed between the clavicular and the middle sternocostal region at any force level (all $p > 0.016$). Similarly, in adduction 60, a *Region* by *Force Level* existed ($F_{2.4, 41.2} = 10.09$, $p < 0.0001$, $\eta^2p = 0.37$). The clavicular region activated more than the superior (all $p < 0.016$), but not the middle sternocostal region (all $p > 0.016$; **Figure 5B**) at all force levels. No differences existed between clavicular and middle sternocostal regions (all $p > 0.016$).

Lastly, in forward flexion and horizontal flexion, a *Region* by *Force Level* interaction existed (forward flexion: $F_{6,48} = 3.29$, $p = 0.009$, $\eta^2p = 0.29$; horizontal flexion: $F_{2,16.6} = 5.65$, $p =$

0.013, $\eta^2p = 0.41$). All three regions activated similarly in both tasks (all $p > 0.016$; **Figure 6**), except in forward flexion at 25% MVF, where the clavicular region activated significantly more than the superior sternocostal region ($p = 0.005$; **Figure 6B**).

DISCUSSION

Pectoralis major differentially activated its fiber regions

Middle sternocostal region was highly activated in isometric internal rotation 90, adduction 90, adduction external 90, and extension. While these humeral tasks were examined in the context of voluntary isometric contractions, they are critical for activities of daily living, such as buttoning a bra (i.e. internal rotation), lowering an object from a shelf (i.e. adduction), opening blinds (i.e. adduction with external rotation), or opening a door (i.e. extension). High normalized activation of the sternocostal regions, specifically in adduction 90 and extension, coincides with normalized regional activations in healthy males (Paton and Brown, 1994). The sternocostal fibers have a mechanical advantage to adduct, internally rotate, or extend the arm (Ackland et al. 2008; Ackland and Pandy, 2011; Wolfe et al. 1992), while the clavicular fibers typically act as an abductor when the arm is elevated at 90° (Ackland et al. 2008). Our findings support and extend these anatomical interpretations, demonstrating essential middle sternocostal region contributions to maintaining exerted forces in adduction, internal rotation, and extension. These current findings may indirectly help explain reported deficits in adduction and extension strength following disinsertion of the lower sternocostal regions in subpectoral breast reconstructions (de Haan et al. 2007; Leonardis et al. 2019).

The clavicular and middle sternocostal regions activated highly in internal rotation and adduction at low arm elevation. The clavicular region's high normalized activation in these tasks

was an unexpected finding. Mechanically, the sternocostal regions have two to three times greater adduction and internal rotation moment arms than the clavicular region (Ackland et al. 2008; Ackland and Pandy, 2011). Therefore, the sternocostal regions should play a major role in the performance of these tasks. However, the clavicular region assists in controlling several joints, including the sternoclavicular, the acromioclavicular, and the glenohumeral joints and its moment generating capability was reported for just the glenohumeral joint (e.g. Ackland et al. 2008; Ackland and Pandy, 2011). Moreover, the magnitude of normalized regional activation quantified in healthy females, specifically in adduction 60, contrasts with healthy males in the same exertion (Paton and Brown, 1994). The normalized EMG amplitudes in healthy males are substantially lower in the clavicular and superior-to-middle sternocostal regions (~6-10%) and appear to have similar activation (Paton and Brown, 1994). Collectively, these findings indicate that females may rely more on activating the clavicular region alongside the middle sternocostal region at low arm elevations. The current mechanism is unclear; however, the clavicular region in females may have divergent neuromuscular control.

Lastly, all three regions had nearly universally high normalized activations in forward and horizontal flexion irrespective of the force level.. This was an unexpected and important finding. The clavicular region has a greater flexor moment arm than the sternocostal region (Ackland et al. 2008), while the clavicular and the superior sternocostal regions have a mechanical advantage to generate horizontal flexion (Kuechle et al. 1997). Logically, higher normalized activations in the clavicular and superior sternocostal regions in these tasks would be anticipated, as previously documented in healthy males (Brown et al. 2007; Paton and Brown, 1994). The contrast may emerge due to differences in sex-specific architectural or neural properties, although anatomical studies did not report sex-related pectoralis major architectural differences (Haladaj et al. 2019).

Alternatively, the contradictory findings may be caused by methodological differences. For example, normalized regional pectoralis major activation in healthy males was acquired with the elbow extended, while all isometric tasks in this study were performed with the elbow flexed. Indeed, regional pectoralis major function highly depends on the elbow joint position (Yu et al. 2011). We purposefully investigated tasks including a flexed elbow because many of the daily tasks require shoulder movement with elbow flexion.

Relevance of differential activation

Pectoralis major fiber regions differentially activated in functionally relevant tasks in females. Several other shoulder muscles are known to differentially activate fiber regions, including the supraspinatus (Alenabi et al. 2019; Calver et al. 2019; Cudlip et al. 2018; Lulic-Kuryllo et al. 2020; Ranjit et al. 2019; Whittaker et al. 2021), infraspinatus (Alenabi et al. 2019; Calver et al. 2019; Lulic-Kuryllo et al. 2020; Ranjit et al. 2019; Whittaker et al. 2021), latissimus dorsi (Brown et al. 2007; Wickham et al. 2012), deltoid (Brown et al. 2007), and subscapularis (Wickham et al. 2014). As in our study, regional activation in these muscles depended on the task, exertion direction, or arm posture. The sternocostal region of the pectoralis major has four to seven partitions (Fung et al. 2009; Wickham et al. 2004), which have divergent pennation angles (Fung et al. 2009) and moment arms (Wickham et al. 2004). Thus, the sternocostal region muscle fiber bundles have distinct lines of action relative to the glenohumeral joint. These lines of action change with arm elevation (Ackland et al. 2008; Pandy and Ackland, 2011), adding an additional layer of functional complexity. Lastly, some studies reported that the clavicular and superior-to-middle sternocostal regions are innervated by at least two sub-branches of the lateral pectoral nerve (Haladaj et al. 2019), which may indicate differential neuromuscular control. This may lead one to hypothesize that the central nervous system employs segmental neuromotor control strategies

to independently control partitions. Considering EMG amplitudes are biased by crosstalk and influenced by many physiological and non-physiological factors (Farina et al. 2004), motor unit data is needed to examine this possibility. Taken together, we hypothesize that this complexity is necessary for the pectoralis major to enable several humeral movements in different arm postures.

LIMITATIONS

Inherent methodological limitations accompany this work. First, HD-sEMG of the inferior sternocostal regions was not acquired due to the overlying breast tissue. The inferior sternocostal region may also activate in specific tasks, such as extension, adduction, and internal rotation, as observed in healthy males (Paton and Brown, 1994). Future studies should consider using fine-wire EMG to evaluate inferior region activation in healthy females. Second, only young females participated, limiting direct translation of findings to other populations. Third, crosstalk from the surrounding muscles, such as the pectoralis minor, subclavius, serratus anterior, external obliques, or intercostal muscles, may have influenced measurements. The degree of crosstalk was minimized by sampling EMG from many closely spaced electrodes and quantifying differential derivation in the post-processing steps. While intermuscular crosstalk was minimized, we cannot eliminate its potential influence of crosstalk at the breast. The influence of the breast tissue on the EMG signal requires further clarification. However, signals were normalized to the maximal voluntary contraction, eliminating some of these effects. Fourth, variations in individual pectoralis major anatomy may have affected data, especially for the middle sternocostal region. Based on the anatomical studies (Fung et al. 2009; Haladaj et al. 2019), the middle sternocostal regions have a greater pennation angle (Fung et al. 2009). Therefore, several HD-sEMG channels located on the lateral aspect of the HD-sEMG array may have sampled parts of the middle sternocostal region. Moreover, the exact number of these channels and location depended on the individual anatomy.

Future work could use imaging tools to distinguish between different partitions of the pectoralis major to improve specificity. Lastly, at least one innervation zone exists within the superior region of the pectoralis major in males (Mancebo et al. 2019). Due to the challenges in quantifying the innervation zones in females, the exact location of these innervation zones was indefinite.

CONCLUSIONS

In conclusion, this work provides the first comprehensive evaluation of the normalized regional pectoralis major activation in healthy females across several tasks involving voluntary isometric ramp and hold contractions. Since these activations differed between tasks, considering the full complexity of the pectoralis major regional contributions in healthy females is warranted. Task divergence of pectoralis major contributions is especially important when considering the design of targeted exercise or rehabilitation interventions. Further, the spatial activation maps generated may be useful for comparisons with compromised populations. In turn, this may enhance development of rehabilitative interventions or exercises to target specific pectoralis major regions.

CONFLICT OF INTEREST STATEMENT

The authors have no conflict of interest that could potentially bias this work.

ACKNOWLEDGEMENTS

The authors would like to thank Bhillie Luciani for her assistance in data collection. This research was partially funded through an NSERC Discovery Grant held by Dr. Clark R. Dickerson (311895-2016). The equipment used was funded through combined support from the Canada Foundation for Innovation and the Ontario Research Fund. Dr. Dickerson is also funded as an NSERC-

sponsored Canada Research Chair in Shoulder Mechanics. Tea Lulic-Kuryllo was supported by the Ontario Graduate Scholarship.

Journal Pre-proofs

References

Ackland D.C., Ponnaren P., Richardson M., Pandy M.G., 2008. Moment arms of the muscles crossing the anatomical shoulder. Journal of Anatomy 213, 383-390.

Ackland D.C., Pandy M.G., 2011. Moment arms of the shoulder muscles during axial rotation. Journal of Orthopaedic Research 29(5), 658-67.

Alenabi T, Whittaker R.L., Kim S.Y., Dickerson C.R., 2019. Arm posture influences on regional supraspinatus and infraspinatus activation in isometric arm elevation efforts. Journal of Electromyography and Kinesiology 44: 108-116.

Ashley G.T., 1952. The manner of insertion of the pectoralis major muscle in man. Anat Rec 113, 301-307.

Brown J.M.M., Wickham J.B., McAndrew D.J., Huang X.-F., 2007. Muscles within muscles: Coordination of 19 muscle segments within three shoulder muscles during isometric motor tasks. Journal of Electromyography and Kinesiology 17, 57-73.

Cabral H.V., de Souza L.M.L., de Oliveira L.F., Vieira T.M., 2021. Non-uniform excitation of the pectoralis major muscle during flat and inclined bench press exercises. Scandinavian Journal of Medicine & Science in Sports.

Calver R., Alenabi T., Cudlip A., Dickerson C.R., Mondal P., Kim S.Y., 2019. Regional activation of supraspinatus and infraspinatus sub-regions during dynamic tasks performed with free weights. Journal of Electromyography and Kinesiology, 102308.

Cudlip A.C., Dickerson C.R., 2018. Regional activation of anterior and posterior supraspinatus differs by place of elevation, hand load and elevation angle. Journal of Electromyography and Kinesiology 43: 14-20.

de Haan A., Toor A., Hage J.J., Veeger H.E.J., Woerdeman L.A.E., 2007. Function of the Pectoralis Major Muscle After Combined Skin-Sparing Mastectomy and Immediate Reconstruction by Subpectoral Implantation of a Prosthesis. Annals of Plastic Surgery 59(6), 605-610.

Drake J.D.M., Callaghan J.P., 2006. Elimination of electrocardiogram contamination from electromyogram signals: An evaluation of currently used removal techniques. Journal of Electromyography and Kinesiology 16(2): 175-187.

Farina D., Merletti R., Enoka R.M., 2004. The extraction of neural strategies from the surface EMG. Journal of Applied Physiology 96(4): 1486-1495.

Fung L., Wong B., Ravichandiran K., Agur A., Rindlisbacher T., Elmaraghy A., 2009. Three-Dimensional Study of Pectoralis Major Muscle and Tendon Architecture. Clinical Anatomy 22: 500-508.

Haladaj R., Wysiadecki G., Clarke E., Polguj M., Topol M., 2019. Anatomical Variations of the Pectoralis Major Muscle: Notes on Their Impact on Pectoral Nerve Innervation Patterns and Discussion on Their Clinical Relevance. BioMed Research International: 6216039.

Joseph R., Alenabi T., Lulic T., Dickerson C.R., 2019. Activation of supraspinatus and infraspinatus partitions and periscapular musculature during rehabilitative elastic resistance exercises. American Journal of Physical Medicine & Rehabilitation 98(5): 407-415.

Kuechle D.K., Newman S.R., Itoi E., Morrey B.F., An K.N., 1997. Shoulder muscle moment arms during horizontal flexion and elevation. Journal of Shoulder and Elbow Surgery 6(5): 429-39.

Leonardis J.M., Lyons D.A., Giladi A.M., Momoh A.O., Lipps D.B., 2019. Functional Integrity of the Shoulder Joint and Pectoralis Major Following Subpectoral Implant Breast Reconstruction. Journal of Orthopaedic Research 37(7): 1610:1619.

Lewis W.H., 1901. Observations on the pectoralis major muscle in man. Bull Johns Hopkins Hosp 12: 172-177.

Lulic-Kuryllo T., Alenabi T., McDonald A.C., Kim S.Y., Dickerson C.R, 2020. Sub-regional activation of supraspinatus and infraspinatus muscles during activities of daily living is task dependent. Journal of Electromyography and Kinesiology 54: 102450.

Lulic-Kuryllo T., Negro F., Jiang N., Dickerson C.R., 2021. Standard bipolar surface EMG estimations mischaracterize pectoralis major activity in commonly performed tasks. Journal of Electromyography and Kinesiology, 56: 102509.

Maganaris C.N., Baltzopoulos V., Sargeant A.J., 2002. Repeated contractions alter the geometry of human skeletal muscle. Journal of Applied Physiology 93(6): 2089-2094.

Mancebo F., Cabral H.V., de Souza L.M.L., de Oliveira L.F., Vieira T.M., 2019. Innervation zone locations distribute medially within the pectoralis major muscle during bench press exercise. Journal of Electromyography and Kinesiology 46: 8-13.

Paton M.E., Brown J.M.M., 1994. An Electromyographic Analysis of Functional Differentiation in Human Pectoralis Major Muscle. Journal of Electromyography and Kinesiology 4(3):161-169.

Setlock C.A., Lulic-Kuryllo T., Leonardis J.M., Kulik M., Lipps D.B., 2021. Age and sex influence the activation-dependent stiffness of the pectoralis major. J Anat 239(2): 479-488.

Wickham J.B., Brown J.M.M., McAndrew D.J., 2004. Muscles within muscles: Anatomical and functional segmentation of selected shoulder joint musculature. Journal of Musculoskeletal Research 8(1): 57-73.

Wickham J.B., Brown J.M., 2012. The function of neuromuscular compartments in human shoulder muscles. Journal of Neurophysiology 107(1): 336-45.

Wickham J., Pizzari T., Balster S., Ganderton C., Watson L., 2014. The variable roles of the upper and lower subscapularis during shoulder motion. Clinical Biomechanics 29(8): 885-891.

Whittaker R.L., Alenabi T., Kim S.Y., Dickerson C.R., 2021. Regional Electromyography of the Infraspinatus and Supraspinatus Muscles During Standing Isometric External Rotation Exercises. Sports Health: 19417381211043849.

Wolfe S.W., Wickiewicz T.L., Cavanaugh J.T., 1992. Rupture of the pectoralis major muscle. An anatomic and clinical analysis. Am J Sports Med 20: 587-593.

Yu J., Ackland D.C., Pandy, M.G., 2011. Shoulder muscle function depends on elbow joint position: An illustration of dynamic coupling in the upper limb. J Biomech 10(7): 1859-1868.

Journal Pre-proofs

Figure captions

Figure 1: The location of the HD-sEMG array and an example of the trapezoidal isometric ramp-and-hold force trace with representative raw HD-sEMG signals. **A:** 64-channel HD-sEMG array overlaying the pectoralis major. The HD-sEMG array was divided into three regions: rows 1 to 2 - clavicular; 3 to 5 - superior sternocostal; and 6 to 8 - middle sternocostal. **B:** An example of the force trace during the trapezoidal isometric ramp-and-hold task and raw HD-sEMG signals from a single trial of a representative participant.

Figure 2: Tasks investigated in Experiment 1 (A) and Experiment 2 (B). **A:** Experiment 1 tasks included adduction at 60° of abduction, which required pulling the arm-cuff (denoted on the Figure) towards the torso; adduction at 90° of abduction, which involved pushing downwards; adduction at 90° of abduction and 90° of external rotation, which involved pushing downwards; and internal rotation at 60° of abduction, which involved medially rotating the forearm towards the torso. **B:** Experiment 2 tasks included: a) extension at 20° of abduction; b) forward flexion at 20° of abduction; c) horizontal flexion at 90° of abduction and 50° of flexion in the transverse plane, and d) internal rotation at 90° of abduction and 20° of internal rotation. Arrows indicate the direction of the force. The arm-cuff and the location of the six-degree-of-freedom transducer are shown in the figure.

Figure 3: Mean normalized (% MVC) EMG amplitude with scatter graph for clavicular, superior, and middle sternocostal regions with scaled mean normalized topographical maps. Black lines in the bars denote means. Bars denote 95% confidence intervals with standard errors. The scatter

points denote each participant's mean normalized regional activation. Asterisks with horizontal bars between scatter graphs indicate significant differences between the regions. PecC is clavicular region; PecSS is superior sternocostal region, and PecSM is middle sternocostal region. In the topographical maps, the blue colour indicates low normalized activation, and the red colour denotes high normalized activation, with the top of the spatial map corresponding to the clavicular region and the bottom of the topographical map corresponding to the middle sternocostal region. The horizontal black lines separate the clavicular, the superior, and the middle sternocostal regions. **A:** Normalized EMG amplitude scatter graphs for internal rotation at 90° of abduction. Note the high normalized activation of the middle sternocostal region irrespective of the force level in both, the scatter graph and the topographical map. **B:** Normalized EMG amplitude scatter graphs for adduction at 90° of abduction. The middle sternocostal region had higher normalized EMG amplitudes than the superior sternocostal region at all force levels. Topographical maps depicted for each force level show high normalized activation of the middle sternocostal region (red colour; bottom of the topographical map) compared to the clavicular and superior sternocostal region.

Figure 4: Mean normalized (% MVC) EMG amplitude with scatter graph for clavicular, superior, and middle sternocostal regions with scaled mean normalized topographical maps corresponding to each force level for adduction external 90 and extension tasks. Black lines in the bars denote means. Bars denote 95% confidence intervals with standard errors. The scatter points denote each participant's mean normalized regional activation. Asterisks with horizontal bars between scatter graphs indicate significant differences between the regions. PecC is clavicular region; PecSS is superior sternocostal region, and PecSM is middle sternocostal region. In the topographical maps, the blue colour indicates low normalized activation, and the red colour denotes high normalized

activation, with the top of the spatial map corresponding to the clavicular region and the bottom of the topographical map corresponding to the middle sternocostal region. The horizontal black lines separate the clavicular, the superior, and the middle sternocostal regions. **A:** Normalized EMG amplitude scatter graphs for adduction 90 external 90. Note the high normalized activation of the middle sternocostal region at all force levels in the scatter graph and the topographical maps. **B:** Normalized EMG amplitude scatter graphs in extension task. The middle sternocostal region activated highly at all force levels.

Figure 5: Mean normalized (% MVC) EMG amplitude with scatter graph for clavicular, superior, and middle sternocostal regions with scaled mean normalized topographical maps corresponding to each force level for internal rotation 60 and adduction 60. Black lines in the bars denote means. Bars denote 95% confidence intervals with standard errors. The scatter points denote each participant's mean normalized regional activation. Asterisks with horizontal bars between scatter graphs indicate significant differences between the regions. PecC is clavicular region; PecSS is superior sternocostal region, and PecSM is middle sternocostal region. In the topographical maps, the blue colour indicates low normalized activation, and the red colour denotes high normalized activation, with the top of the spatial map corresponding to the clavicular region and the bottom of the topographical map corresponding to the middle sternocostal region. The horizontal black lines separate the clavicular, the superior, and the middle sternocostal regions. **A:** Normalized EMG amplitude scatter graphs for internal rotation at 60° of abduction. Note the high normalized activation of the clavicular and the middle sternocostal regions at all force levels as shown in the scatter graph and the topographical maps. **B:** Normalized EMG amplitude scatter graphs for

adduction at 60°. The clavicular region activated more than the superior but not the middle sternocostal region across force levels.

Figure 6: Mean normalized (% MVC) EMG amplitude scatter graphs for clavicular, superior, and middle sternocostal regions with scaled mean normalized topographical maps corresponding to each force level for forward flexion and horizontal flexion. Black lines in the bars denote means. Bars denote 95% confidence intervals with standard errors. The scatter points denote each participant's mean normalized regional activation. Asterisks between scatter graphs indicate significant differences between the regions. PecC is clavicular region; PecSS is superior sternocostal region, and PecSM is middle sternocostal region. In the topographical maps, the blue colour indicates low normalized activation, and the red colour denotes high normalized activation, with the top of the spatial map corresponding to the clavicular region and the bottom of the topographical map corresponding to the middle sternocostal region. The horizontal black lines separate the clavicular, the superior, and the middle sternocostal regions. **A:** Normalized EMG amplitude scatter graphs for horizontal flexion. All three regions activated similarly across force levels, which is visualized in the topographical maps. **B:** Normalized EMG amplitude scatter graphs for forward flexion. All three regions activated similarly across force levels, except in 25% MVF, where the clavicular region activated more than the super sternocostal region.

Journal Pre-proofs

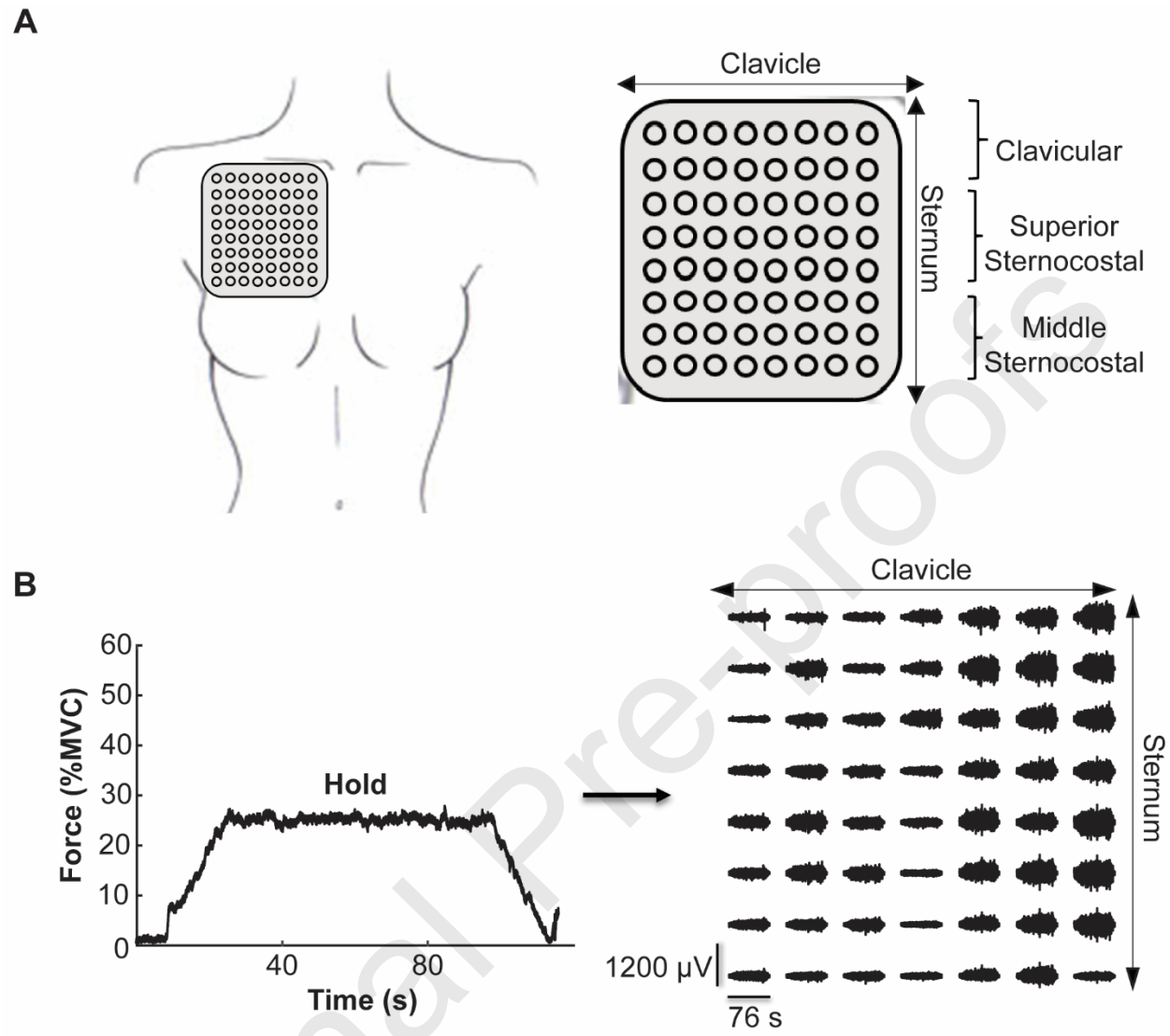

Journal Pre-proofs

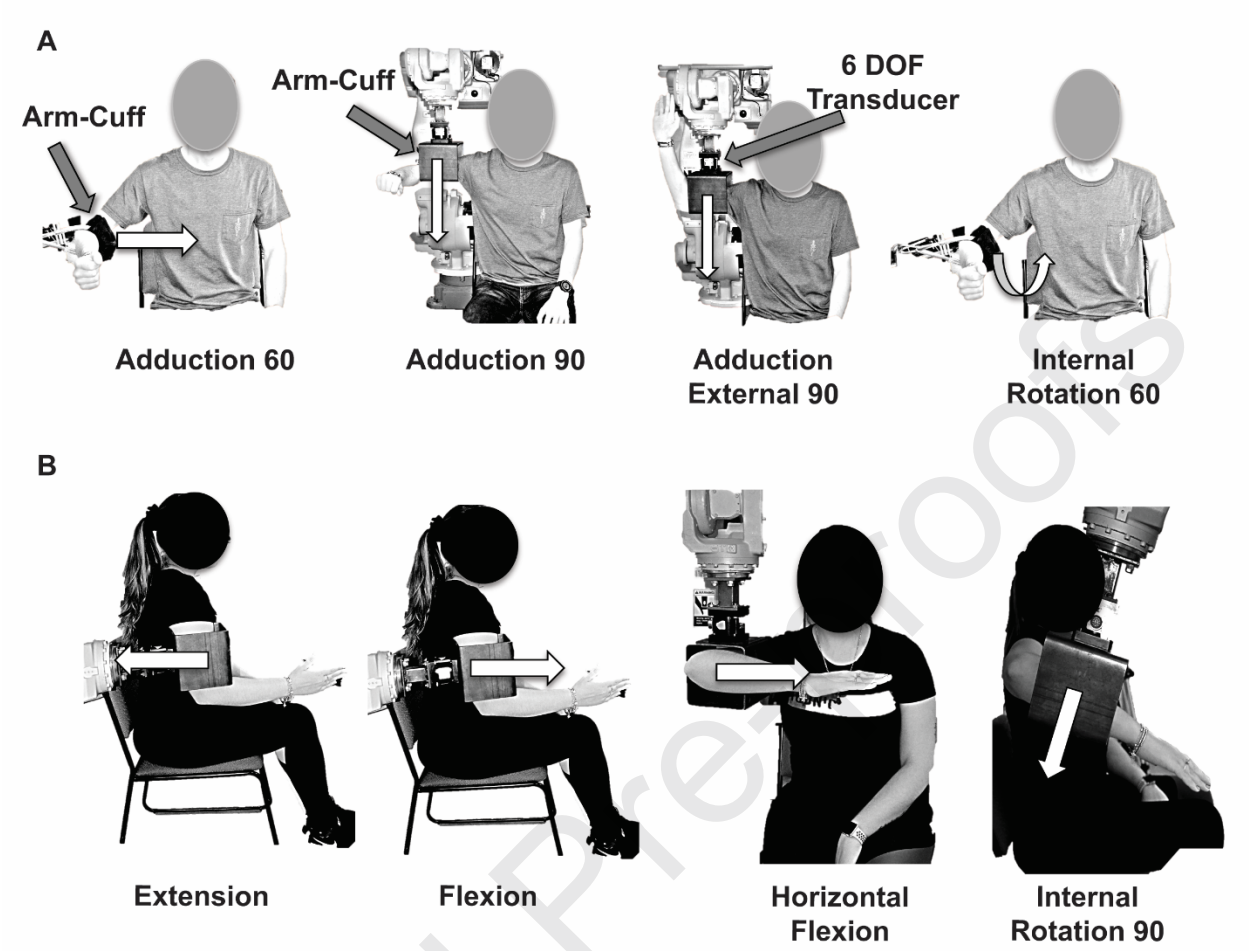

Journal Pre-proofs

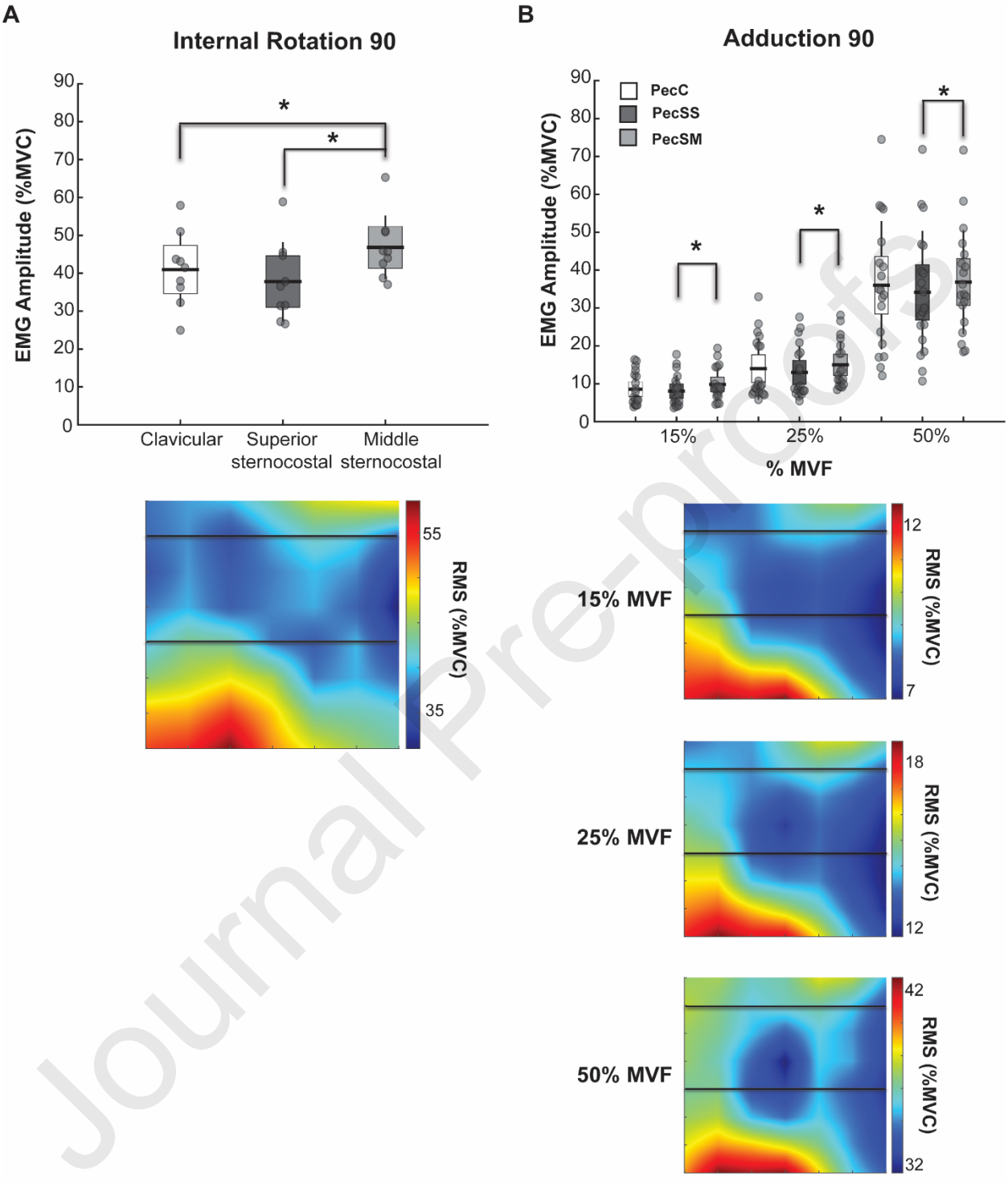

Journal Pre-proofs

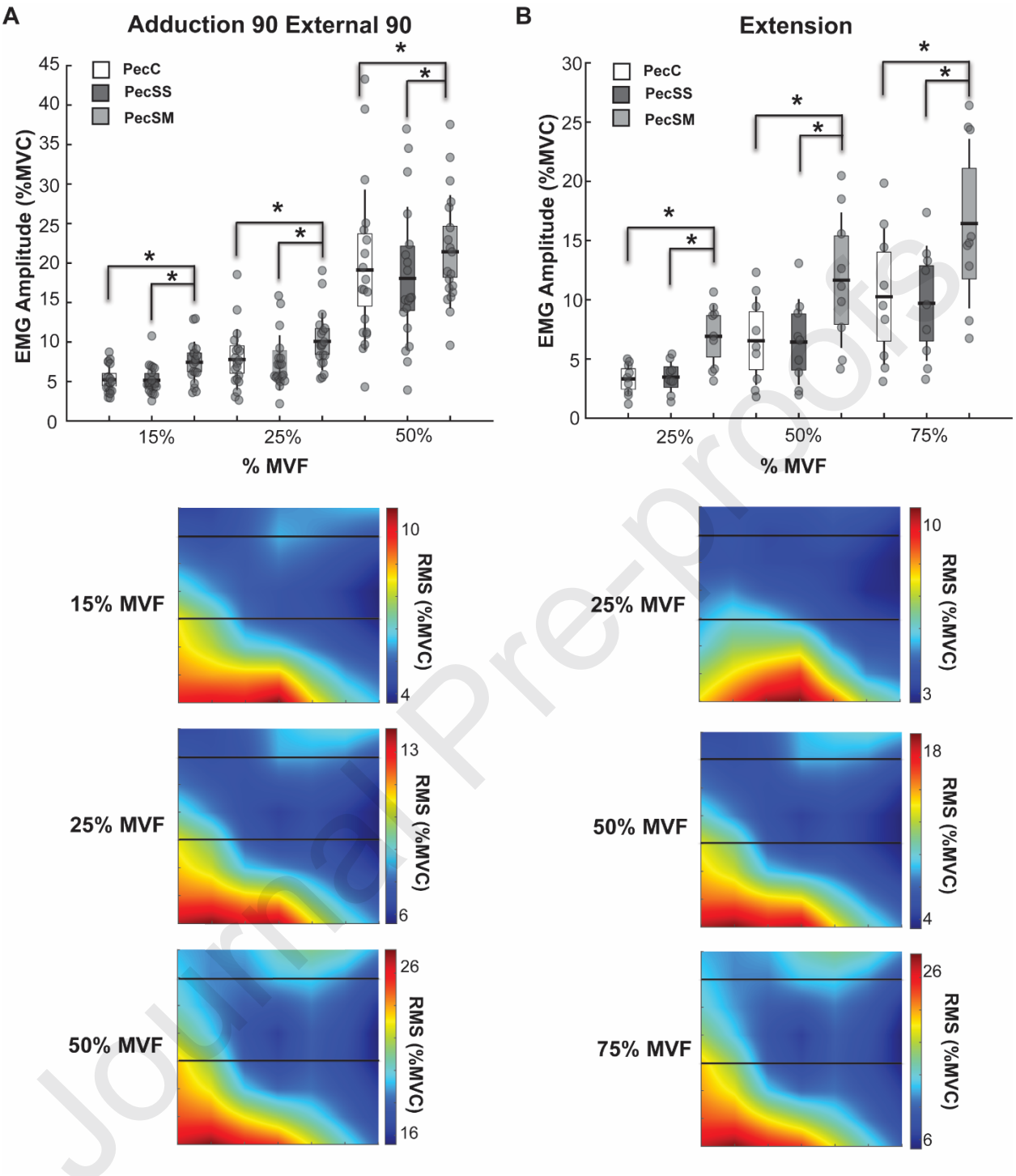

Journal Pre-proofs

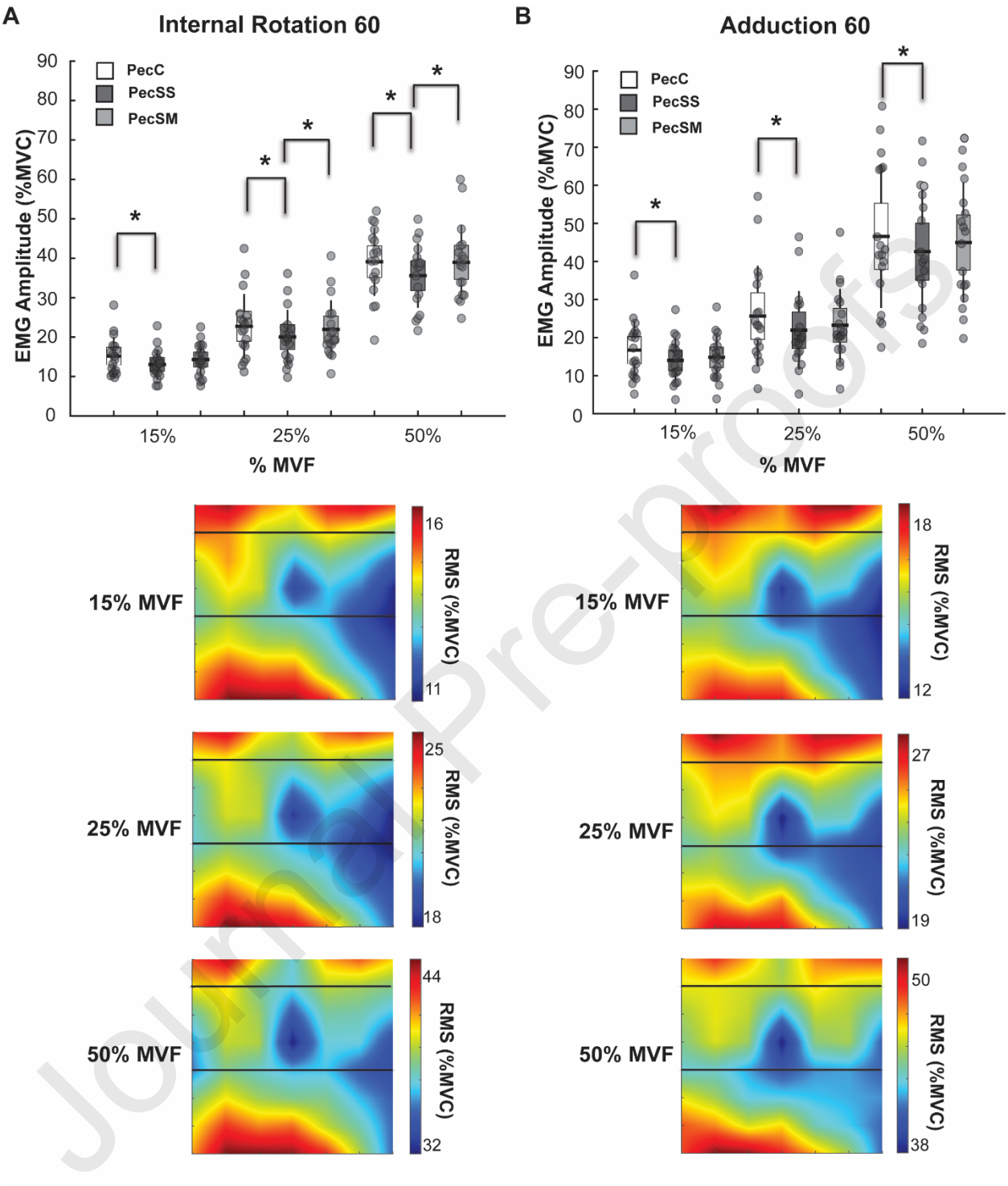

Journal Pre-proofs

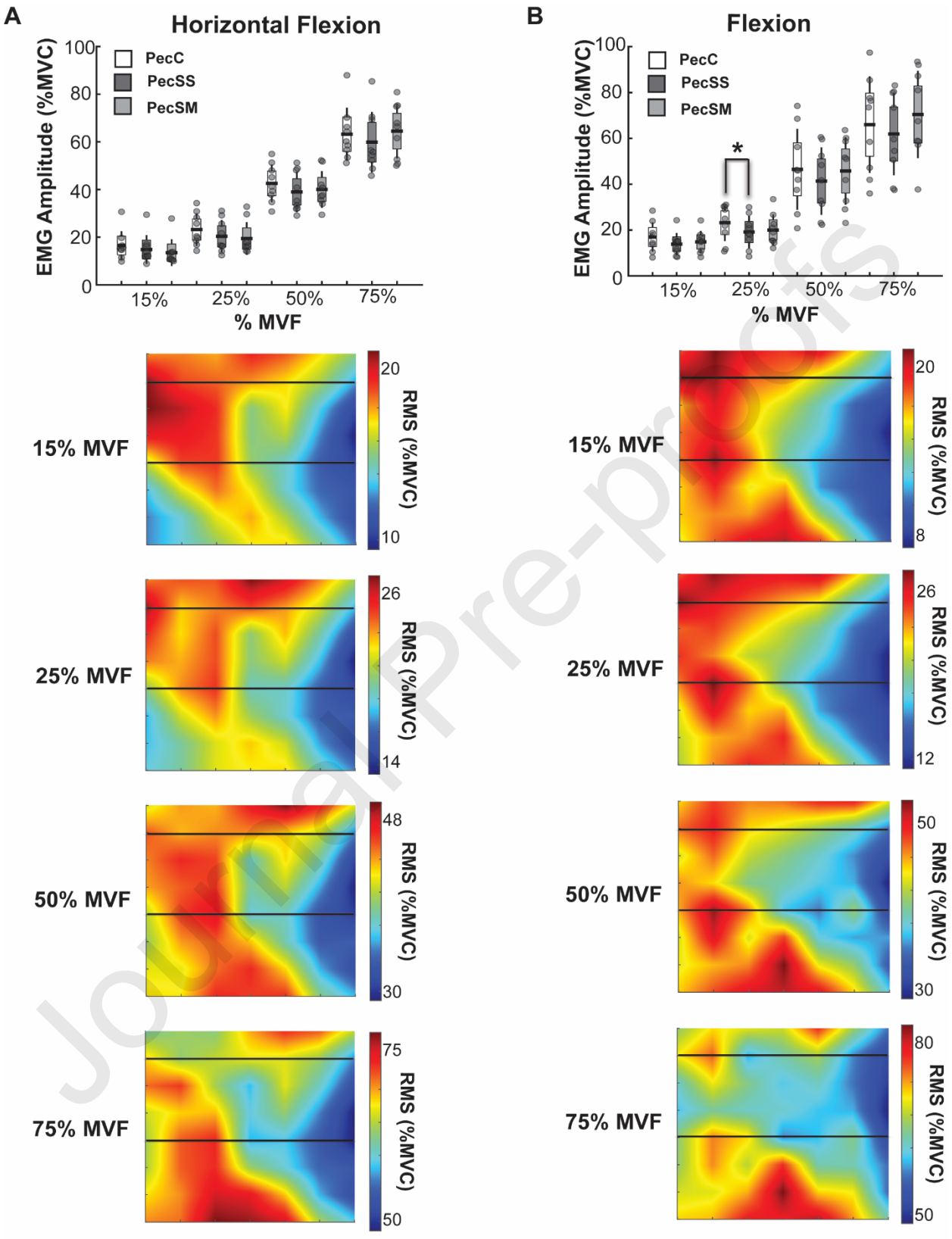

Journal Pre-proofs